



Research Paper

Binding Energy in Tuned Quantum Dots under an External Magnetic Field

Pariya Hashemi¹, Mojtaba Servatkhan^{*1,2}, Raheleh Pourmand³,
Vahid Setoodeh^{1,2}.

¹ Department of Physics, Marvdasht Branch, Islamic Azad University, Marvdasht, Iran

² Department of Physics, Nanotechnology Research Center, Marvdasht Branch, Islamic Azad University, Marvdasht, Iran

³ Department of Physics, Estahban Higher Education Center, Estahban 74519-44655, Iran

Received: 3 Sep. 2022

Revised: 20 Oct. 2022

Accepted: 10 Nov. 2022

Published: 20 Nov. 2022

Use your device to scan
and read the article online



Keywords:

Majority Gate, Decoder,
Reliability, Fault
Tolerant, Quantum-dot
Cellular Automata,
Coplanar

Abstract The ground state binding energy of a tuned quantum dot (QD) under an external magnetic field has been theoretically investigated. For this goal, the Schrödinger equation is analytically solved without and with considering the central impurity term and the energy eigenvalues and eigenfunctions are analytically derived. Then, the binding of the tuned QD was studied considering the various parameters. We found that (i) the binding energy decreases by rising the potential range. (ii) The binding energy reduces with enhancing the potential depth. (iii) The binding energy increases with rising the magnetic field and the confinement frequency. The depth and stretching range of the confinement potential have important effects on the binding energy of the tuned QD.

Citation: ParyaHashemi, Mojtaba Servatkhan, Raheleh Pourmand, Vahid Setoodeh.
Binding Energy in Tuned Quantum Dots under an External Magnetic Field.

Journal of Optoelectrical Nanostructures. 2022; 7 (4): 49-65

DOI: [10.30495/JOPN.2022.30924.1270](https://doi.org/10.30495/JOPN.2022.30924.1270)

***Corresponding author:** Dr.Mojtaba Servatkhan.

Address: Department of Physics, Marvdasht Branch, Islamic Azad University, Marvdasht, Iran. **Tell:** 07191300012 **Email:** servatkhan@miau.ac.ir.

1. INTRODUCTION

The physical properties of semiconductor nanostructures are particularly fascinating and essential in potential applications. The quantum dots (QDs) have drawn the attention of many scientists during the past two decades [1-6]. The electron energy levels in the structures can be manipulated by changing their parameters.

The knowledge of the physical properties of nanostructures is an interesting problem in physics and engineering. The theoretical information about the electronic and optical properties of nanostructures can be employed in designing optoelectronic devices [7-10].

Hitherto, many studies were performed on the electronic properties of different nanostructures without considering impurity states by using different confinement potentials [11-17]. The subject of determining the electronic properties of nanostructures based on information about confinement potential has been attended to [13-16]. So far, the QDs with different shapes have been considered in the literature, like the sphere, Gaussian, Wedge-shaped, V-shaped, square, etc. [17-24]. For some confining potentials in QDs, there is no analytical solution to the Schrödinger equation. In this case, other numerical methods are employed such as perturbation, the WKB method, variation, factorization, and diagonalization [25-29].

Among the electronic properties, the binding energy has an important role in physics. The determination of energy states considering the impurity effect can be used in industrial applications. The influences of external factors on the binding have been investigated in the past three decades. For instance, Elward *et al.* [30] studied the binding energy in CdSe QDs considering electron-hole recombination. Merchancano *et al.* [31] investigated the binding energy of a donor in GaAs QDs under pressure. The readers can refer to [32-36].

Here, the ground state binding energy of a tuned QD was calculated under various parameters. To this end, the Schrödinger equation analytically is solved and the energy eigenvalues and eigenfunctions were derived. Then, we study the influences of an external magnetic field, and QD size on the binding energy of the system.

The paper is structured as follows. In Sec. 2, we presented the calculation method of the eigenvalues and eigenstates of the system. Also, the binding energy calculation has been presented. The results have been shown in Sec. 3. The conclusion has been presented in Sec. 4 majority gate, its functionality verification, and reliability analysis are studied in Section 3. Section 4 introduces a robust 2-to-4 decoder based on the proposed majority gate. Finally, we conclude in Section 5.

2. THEORETICAL METHOD

The Hamiltonian of a charge carrier at the QD under a magnetic field B is expressed by

$$H = \frac{1}{2m^*} (\mathbf{P} + e\mathbf{A})^2 + V(\mathbf{r}) \quad (1)$$

Here, e and m^* are the electron charge and effective mass, respectively. In the above equation, $\mathbf{A} = \frac{Br}{2} \boldsymbol{\varphi}$, and $V(r) = V_1(r) + V_2(r)$ is the confining potential. The first and second terms are expressed by [37-41]

$$\begin{aligned} V_1(r) \\ = \frac{1}{2} m^* \omega_0^2 r^2 + \frac{\hbar^2}{2m^*} \frac{\xi}{r^2}. \end{aligned} \quad (2)$$

And

$$V_2(r) = -V_0 \exp \left[- \left(\frac{r}{R_0} \right)^q \right]. \quad (3)$$

Where ξ is a dimensionless parameter, V_0 and R_0 are the depth and range of the potential. Here, it is considered $q = 2$ and $r/R_0 \ll 1$. Therefore, we have

$$V_2(r) = -V_0 \left[1 - \left(\frac{r}{R_0} \right)^2 \right] \quad (4)$$

Considering the model mentioned above, the energy eigenvalues and eigenfunctions can be obtained. The total Hamiltonian of the system is given by

$$\begin{aligned} H = -\frac{\hbar^2}{2m^*} \left(\frac{\partial^2}{\partial r^2} + \frac{1}{r} \frac{\partial}{\partial r} + \frac{1}{r^2} \frac{\partial^2}{\partial \varphi^2} \right) + \frac{1}{2} m^* \left(\omega_0^2 + \frac{\omega_c^2}{4} + \frac{2V_0}{m^* R_0^2} \right) r^2 - V_0 \\ - i\hbar \frac{\omega_c}{2} \frac{\partial}{\partial \varphi} + \frac{\hbar^2}{2m^*} \frac{\xi}{r^2} \end{aligned} \quad (5)$$

where $\omega_c = \frac{eB}{m^*}$. To solve the Schrödinger equation, we select the following relation

$$\Psi(r, \varphi) = X(r) \frac{e^{im\varphi}}{\sqrt{2\pi}} \quad (6)$$

Using Eq. (6), we have

$$\frac{d^2X(r)}{dr^2} + \frac{1}{r} \frac{dX(r)}{dr} + \left[\alpha^2 - \frac{\beta^2}{r^2} - \Omega^2 r^2 \right] X(r) = 0 \quad (7)$$

where α , β , and Ω are defined as

$$\alpha^2 = \frac{2m^*(E + V_0)}{\hbar^2} - \frac{meB}{\hbar} \quad (8)$$

$$\beta^2 = m^2 + \xi \quad (9)$$

$$\Omega^2 = \frac{2m^*V_0}{\hbar^2 R_0^2} + \frac{e^2 B^2}{4\hbar^2} + \frac{m^{*2} \omega_0^2}{\hbar^2} \quad (10)$$

The below relation is employed

$$X(r) = r^\beta e^{-\frac{\Omega r^2}{2}} h(r), \quad (11)$$

And also $x = \Omega r^2$. It yields

$$\frac{d^2h(x)}{dx^2} + [\beta - x + 1] \frac{dh(x)}{dx} + nh(x) = 0 \quad (12)$$

The solution is denoted by $h(x) = L_n^\beta(x)$. Also, n is an integer and is expressed as

$$n = \frac{\alpha^2}{4\Omega} - \frac{\beta + 1}{2} \quad (13)$$

Using Eqs. (6), (11), and (12), the wave function is as follows

$$\Psi(r, \varphi) = Ar^\beta e^{-\frac{\Omega r^2}{2}} F(-n, \beta + 1; \Omega r^2) e^{im\varphi} \quad (14)$$

where $F(-n, \beta + 1; \Omega r^2)$ is the confluent hypergeometric function, A is the normalization constant as

$$A = \frac{1}{n! \sqrt{\frac{\Omega^{\beta+1} (n + \beta)!}{\pi n!}}} \quad (15)$$

Employing Eq. (13), we obtain the energy eigenvalues as

$$E_{n,m} = \frac{\hbar^2}{m^*} \left(2n + \sqrt{m^2 + \xi} + 1 \right) \sqrt{\frac{2m^*V_0}{\hbar^2 R_0^2} + \frac{e^2 B^2}{4\hbar^2} + \frac{m^{*2} \omega_0^2}{\hbar^2}} + \frac{meB\hbar}{2m^*} - V_0 \quad (16)$$

2.1. IMPURITY EFFECT

The system is considered in the presence of a hydrogenic impurity. The Schrödinger is written as [41]

$$H(r)\Phi_{n,m}(r) = \left[H_0(r) + \frac{\kappa k}{r} \right] \Phi_{n,m}(r) = \epsilon_{n,m} \Phi_{n,m}(r) \quad (17)$$

where $k = -\frac{e^2}{4\pi\epsilon\epsilon_0}$. Also, $\kappa = 1$ ($\kappa = -1$) related to donor (acceptor) impurity. In Eq. (17), $\epsilon_{n,m}$, and $\Phi_{n,m}$ are the energy eigenvalues and eigenfunctions of the perturbed system. The energy eigenvalues in the presence of the impurity is

$$\epsilon_{n,m} = E_{n,m} - \langle \Psi_{n,m} | H(r) | \Psi_{n,m} \rangle \quad (18)$$

Where $\Psi_{n,m}$ is the wave function without impurity.

Using Eqs. (14) and (16), the energy under the impurity effect is

$$\epsilon_{n,m} = \frac{\hbar^2}{m^*} \left(2n + \sqrt{m^2 + \xi} + 1 \right) \sqrt{\frac{2m^*V_0}{\hbar^2 R_0^2} + \frac{e^2 B^2}{4\hbar^2} + \frac{m^{*2} \omega_0^2}{\hbar^2}} + \frac{meB\hbar}{2m^*} - V_0 - k \sqrt{\frac{m^* \Omega}{\hbar}} \frac{1}{\sqrt{2n + 1 + \sqrt{m^2 + \xi}}} \quad (19)$$

The binding energy is an important quantity in physics and chemistry. Here, we define the binding energy as

$$E_b = E_{without\ impurity} - E_{with\ impurity}$$

The binding energy is amount of energy required to separate a particle from a system of particles or to disperse all the particles of the system.

3. RESULTS AND DISCUSSION

In this part, all theoretical calculations are performed for a GaAs QD with the following parameters: $m^* = 0.067m_0$ and $\epsilon = 12.4\epsilon_0$.

Fig. 1 display the ground state binding energy versus the dimensionless parameter ξ for $B=5$ T, $V_0=300$ meV, $\omega_0 = 200$ THz and $R_0=10$ nm. It is clear that the binding energy reduces with increasing the ξ parameter. It is observed that the highest binding energy corresponds to $\xi = 0$ which relates to a 2D quantum disk. When ξ increases, the repulsive potential enhances at the center of the system. Hence, the distance between electron and impurity rises and the binding energy decreases. An increase in ξ causes the repulsive potential at the QD center. Thereby, the electron is more confined. We can say that with adjusting this parameter, the electron confinement is changed.

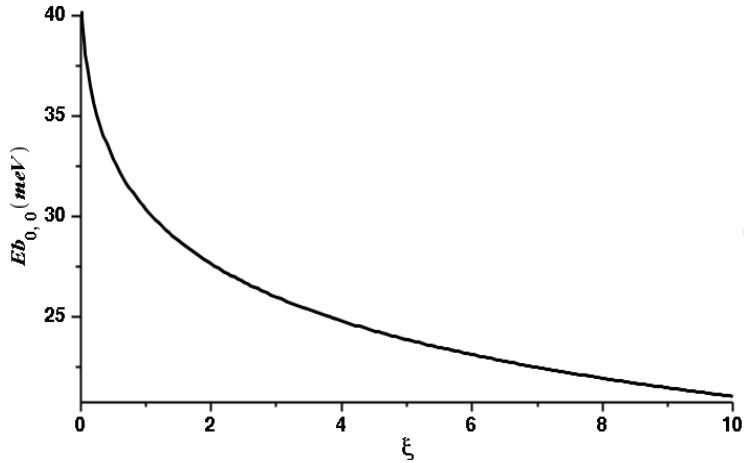


Fig. 1. The ground state binding energy versus the dimensionless parameter ξ .

In Fig. 2, variations of the ground state binding energy have been plotted versus the dimensionless parameter ξ for different confinement frequencies, $\omega_0 = 300, 500, 700$ THz, with $B=5$ T, $V_0=300$ meV, and $R_0=10$ nm. It is seen that the binding energy reduces with increasing the ξ parameter. As can be seen, the binding energy increases by rising the confinement frequency at a fixed value of ξ .

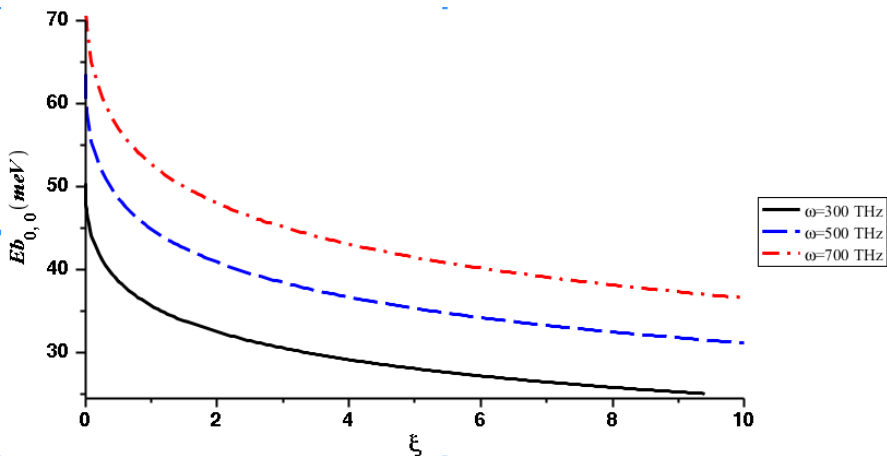


Fig. 2. The ground state binding energy versus the dimensionless parameter ξ for different confinement frequencies

Binding Energy in Tuned Quantum Dots under an External Magnetic Field

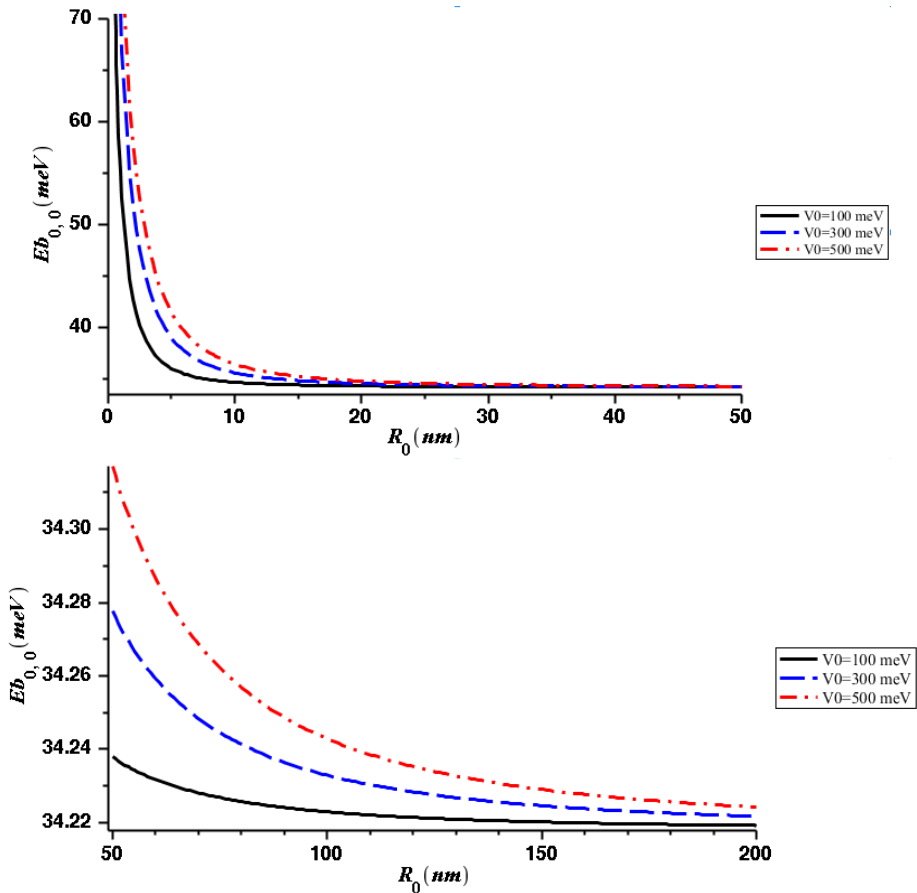


Fig. 3. The ground state binding energy versus R_0 for different ranges of $R_0 = 0 - 50$ THz and $R_0 = 5-200$ THz

In Fig. 3, the variations of the ground state binding energy with the range of potential R_0 are plotted for different potential depths with $B=5$ T, $\xi = 1$, and $\omega_0=300$ THz. With rising the potential range, the binding energy decreases. With increasing the potential range, the wave function extends a greater region thereby the distance between electron and impurity rises. This means that the binding energy reduces. Also, the binding energy increases with enhancing the potential depth at a fixed potential range. It is also seen that all lines (Black, Blue, Red) tends to the same values when the radius is greater than 20 nm. To compare the

difference between the values of the binding energy for larger values of R_0 , the ground state binding energy with the range of potential $R_0 = 50 - 200 \text{ nm}$ are plotted. It is seen that there is a slight difference between the values of binding energy for different values of confinement potential. This difference decrease from about 0.04 meV for $R_0 = 50 \text{ nm}$ to less than 0.01 meV for $R_0 = 200 \text{ nm}$.

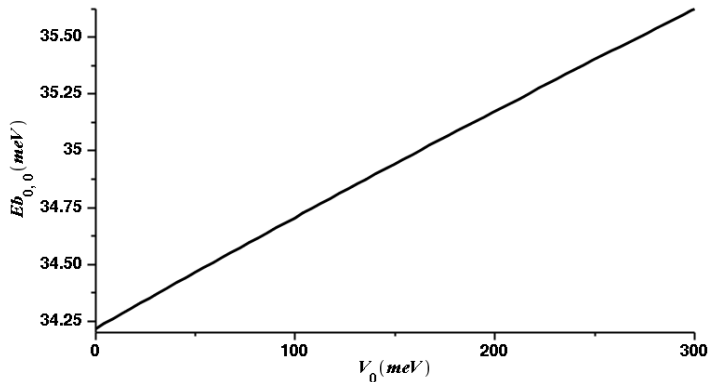


Fig. 4. The ground state binding energy versus depth of potential V_0 .

Fig. 4 shows the variations of the ground state binding energy with the depth of potential V_0 for $B=5 \text{ T}$, $\xi = 1$, $\omega_0=300 \text{ THz}$, and $R_0=10 \text{ nm}$. With increasing the potential depth, the binding energy increases. When the potential depth increases, the bottom of the well shifts toward lower energies and the energy of confined states increases. Hence, the distance between the electron and impurity decreases thereby the binding energy increases. With rising V_0 , the slope of potential function versus r produces a great confinement on the electron. Therefore, the binding energy is increased.

Fig. 5 demonstrates the ground state binding energy versus the magnetic field for different potential depths with $R_0=10$ nm, $\omega_0=10$ THz, and $\xi = 1$. The binding energy increases with rising the magnetic field. It should be noted that the magnetic field has two effects. It creates parabolic confinement and a displacement of energy towards higher or lower energies (see Eq. (19)). This displacement does not exist for the ground state binding energy. When the magnetic field increases, the confinement rises and the electron wave function is localized in a smaller region. Therefore, the distance between the electron and impurity reduces and the binding energy increases.

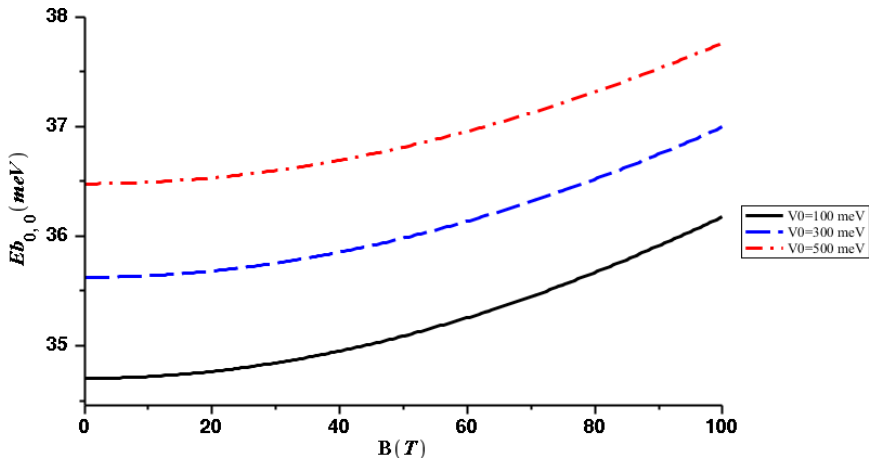


Fig. 5. The ground state binding energy versus magnetic field for different depth of potential V_0 .

In Fig. 6, the variations of the ground state binding energy with the confinement frequency ω_0 are plotted for different potential depths with $B=5$ T, $\xi = 1$, and $R_0=10$ nm. As can be seen, the binding energy increases with rising the confinement frequency. With increasing the confinement frequency, the wave function extends a smaller region thereby the distance between electron and impurity reduces. This means that the binding energy increases.

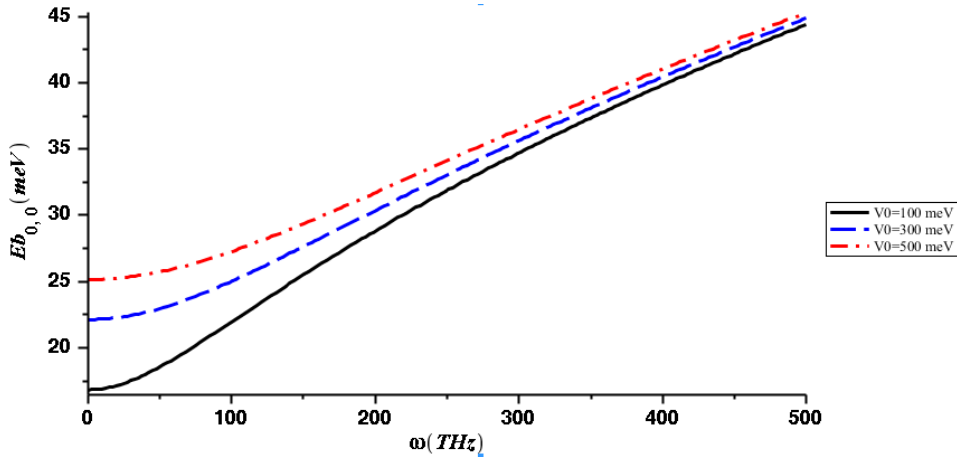


Fig. 6. The ground state binding energy versus confinement frequency for different potential depths.

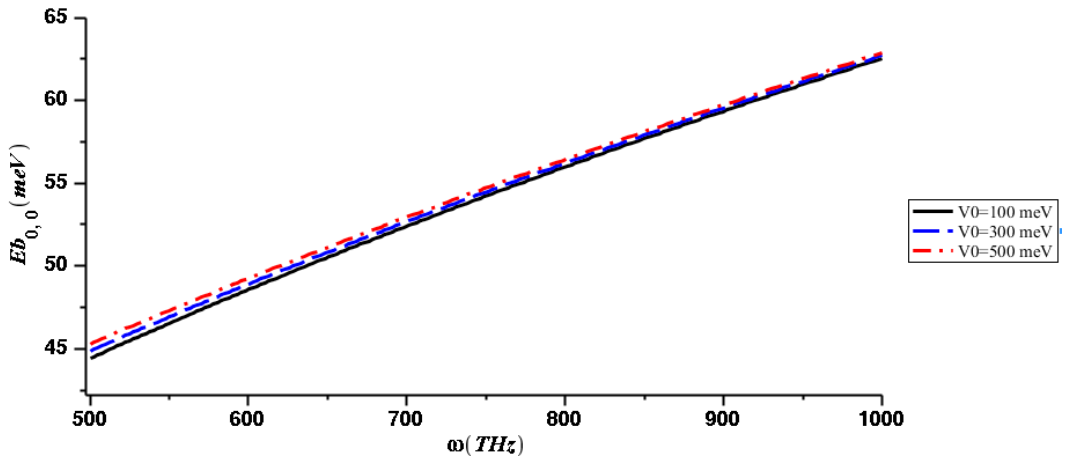


Fig. 7. The ground state binding energy versus confinement frequency (500-1000 THz) for different potential depths.

Fig. 7, like Fig. 6, shows the variations of the ground state binding energy with the confinement frequency ω_0 (but in the range of 500-1000 THz) for different potential depths with $B=5$ T, $\xi = 1$, and $R_0=10$ nm. As can be seen, the binding energy increases with rising the confinement frequency. With increasing the confinement frequency more than 500 THz all the lines (black, Blue, Red) tends to the same value and show a linear growth.

4. CONCLUSION

In this study, a tuned QD is considered under an applied magnetic field and a hydrogenic donor impurity at the center of QD. The binding energy of the system has been calculated for different parameters. To this goal, the Schrödinger equation is analytically solved and the energy eigenvalues and eigenstates are derived. We aim to show the effects of various parameters on the ground state binding energy of the system. The results reveal that the consideration of different parameters has an important effect on the binding energy. We could not find experimental data to compare our theoretical results with available data.

CONFLICT OF INTEREST

The authors state that publication of this manuscript does not involve any conflicts of interest.

REFERENCES

- [1] Khanonkin I, Bauer S, Mikhelashvili V, Eyal O, Lorke M, Jahnke F, Reith Maier J. P, Eisenstein G, On the principle operation of tunneling injection quantum dot lasers. *Prog Quant Electron* 81 (2022) 100362.
<https://doi.org/10.1016/j.pquantelec.2021.100362>.
- [2] Dusanowski L, Nawrath C, Portalupi S. L, Jetter M, Huber T, Klemmt S, Michler P, Hofling S, Optical charge injection and coherent control of a quantum-dot spin-qubit emitting at telecom wavelengths. *Nature Commun* 13 (2022) 748.
<https://doi.org/10.1038/s41467-022-28328-2>
- [3] Ali A. A, Shaer A, Elsaid M, Simultaneous effects of Rashba, magnetic field and impurity on the magnetization and magnetic susceptibility of a GaAs-semiconductor quantum ring. *J Magn Magn Matter* 556 (2022) 169435.
<https://doi.org/10.1016/j.jmmm.2022.169435>
- [4] Thakur T, Szafran B, Aharonov-Bohm oscillations in phosphorene quantum rings: Mass anisotropy compensation by confinement potential. *Phys Rev B* 105 (2022) 165309.
<https://doi.org/10.1103/PhysRevB.105.165309>
- [5] Rastegar Sedehi H. R, Khordad R, Bahramiyan H, Optical properties and diamagnetic susceptibility of a hexagonal quantum dot: impurity effect. *Opt Quant Electron* 53 (2021) 264.
<https://doi.org/10.1007/s11082-021-02927-7>
- [6] Avazzadeh Z, Bahramiyan H, Khordad R, Mohammadi S. A, Diamagnetic susceptibility of an off-center hydrogenic donor in pyramid-like and cone-like quantum dots. *Eur Phys J Plus* 131 (2016) 121.
<https://doi.org/10.1140/epjp/i2016-16121-8>
- [7] Nasrallah S, Sfina N, Said M, Electronic properties of intersubband transition in (CdS/ZnSe)/BeTe quantum wells. *Eur Phys J B* 47 (2005) 167-170.
<https://doi.org/10.1140/epjb/e2005-00323-0>
- [8] Imamura K, Sugiyama Y, Nakata Y, Muto S, Yokoyama N, New optical memory structure using self-assembled InAs quantum dots. *Jpn J Appl Phys* 34 (1995) L1445.
<https://doi.org/10.1143/JJAP.34.L1445>

- [9] E. Leobandung, L. Guo, S. Y. Chou, Single hole quantum dot transistors in silicon. *Appl. Phys. Lett.* 67 (1995) 2338.
<https://doi.org/10.1063/1.114337>
- [10] Durante F, Alves P, Karunasiri G, Hanson N, Byloos M, Liu H. C, Bezinger A, Buchanan M, NIR, NWIR and LWIR quantum well infrared photodetector using interband and intersubband transitions. *Infrared Phys Technol* 50 (2007) 182-186.
<https://doi.org/10.1016/j.infrared.2006.10.021>
- [11] Khordad R, Optical properties of quantum wires: Rashba effect and external magnetic field. *J Lumin* 134 (2013) 201.
<https://doi.org/10.1016/j.jlumin.2012.08.047>
- [12] Lu L, Xie W, Hassanabadi H, The effects of intense laser on nonlinear properties of shallow donor impurities in quantum dots with the Woods-Saxon potential. *J Lumin* 131 (2011) 2538.
<https://doi.org/10.1016/j.jlumin.2011.06.051>
- [13] Hashemi P, Servatkah M, Pourmand R, The effect of Rashba spin-orbit interaction on optical far-infrared transition of tuned quantum dot/ring systems. *Opt Quant Electron* 53 (2021) 567.
<https://doi.org/10.1007/s11082-021-03173-7>
- [14] Khordad R, Rastegar Sedehi H. R, Electrocaloric effect in quantum dots using the non-extensive formalism. *Opt Quant Electron* 53 (2021) 264.
<https://doi.org/10.1007/s11082-022-03902-6>
- [15] Ghanbari A, Khordad R, Bound states and optical properties for Derjaguin-Landau-Verweij-Overbook potential. *Opt Quant Electron* 53 (2021) 152.
<https://doi.org/10.1007/s11082-021-02797-z>
- [16] Sayrac M, Effects of applied external fields on the nonlinear optical rectification, second, and third-harmonic generation in an asymmetrical semi exponential quantum well. *Opt Quant Electron* 54 (2022) 52.
<https://doi.org/10.1007/s11082-021-03425-6>
- [17] Holovatsky V, Chubrey M, Voitsekhivska O, Effect of electric field on photoionization cross-section of impurity in multilayered quantum dot. *Superlatt Microstrut* (2022) 107137.

<https://doi.org/10.1016/j.spmi.2020.106642>

- [18] Sayari A, Servatkhah M, Pourmand R, Effects of electron-phonon interaction and pressure on optical properties of wedge-shaped quantum dots. *Physica B* 628 (2022) 413631.

<https://doi.org/10.1016/j.physb.2021.413631>

- [19] Servatkhah M, Pourmand R, Optical properties of a two-dimensional GaAs quantum dot under strain and magnetic field. *Eur Phys J Plus* 135 (2020) 754.

<https://doi.org/10.1140/epjp/s13360-020-00773-2>

- [20] Khordad R, Vaseghi B, Effects temperature, pressure and spin-orbit interaction simultaneously on third harmonic generation of wedge-shaped quantum dots. *Chin J Phys* 59 (2019) 473-480.

<https://doi.org/10.1016/j.cjph.2019.04.005>

- [21] Kirak M, Magnetic and thermodynamic properties of GaAs quantum dot confined by parabolic-inverse square plus Gaussian potential. *J Magn Magn Mater* 536 (2021) 167481.

<https://doi.org/10.1016/j.jmmm.2020.167481>

- [22] Khordad R, Bahramiyan H, *Int J Mod Phys C* 24 (2013) 1350041.

- [23] Hayek L. A, Sandouqa A. S, Energy and binding energy of donor impurity in quantum dot with Gaussian confinement. *Superlatt Microstruct* 85 (2015) 216.

<https://doi.org/10.1016/j.spmi.2015.05.025>

- [24] Khordad R, Effect of temperature on the binding energy of excited states in a ridge quantum wire. *Physica E* 41 (2009) 543-547.

<https://doi.org/10.1016/j.physe.2008.10.004>

- [25] Ungan F, Bahar M. K, Pal S, Romas M. E. M, Electron-related nonlinear optical properties of cylindrical quantum dot with the Rosen-Morse axial potential. *Commun Theor Phys* 72 (2020) 075505.

<https://doi.org/10.1088/1572-9494/ab8a1d>

- [26] Firoozi A, Mohammadi A, Khordad R, Jalali T, Q-BOR-FDTD method for solving Schrodinger equation for rotationally symmetric nanostructures with hydrogenic impurity. *Phys Script* 97 (2022) 025802.

<https://doi.org/10.1088/1402-4896/ac48ac>

- [27] Bose C, Perturbation calculation of impurity states in spherical quantum dots with parabolic confinement. *Physica E* 4 (1999) 180-184.
[https://doi.org/10.1016/S1386-9477\(99\)00010-7](https://doi.org/10.1016/S1386-9477(99)00010-7)
- [28] Ikhdair S. M, Sever R, Approximate eigenvalue and eigenfunction solutions for the generalized Hulthen potential with any angular momentum. *J Math Chem* 42 (2007) 461-471.
<https://doi.org/10.1007/s10910-006-9115-8>
- [29] Bose C, Sarkar C. K, Perturbation calculation of donor states in spherical quantum dots. *Solid State Electron* 42 (1998) 1661-1663.
[https://doi.org/10.1016/S0038-1101\(98\)00126-9](https://doi.org/10.1016/S0038-1101(98)00126-9)
- [30] Elward J. M, Chakraborty A, Effect of dot size on exciton binding energy and electron-hole recombination probability in CdSe quantum dots. *J Chem Theory Comput* 9 (2013) 4351-4359.
<https://doi.org/10.1021/ct400485s>
- [31] Merchancano S. T. P, Marinez L. E. B, The binding energy of donor impurities in GaAs quantum dots under the pressure effect. *Rev Mex de Fis* 53 (2007) 470-474.
- [32] Mikhail I. F. I, El Sayed S. B. A, Exact and variational calculations of a hydrogenic impurity binding energy in a multilayered spherical quantum dot. *Physica E* 43 (2011) 1371.
<https://doi.org/10.1016/j.physe.2011.03.007>
- [33] Hashemi P, ServatkhahM, Pourmand R, *Opt Commun* 506 (2022) 127551.
- [34] Jahan K. L, Boda A, Shankar I. V, Raju Ch. N, Chatterjee A, Magnetic field effect on the energy levels on an exciton in a GaAs quantum dot: Application for excitonic lasers. *Sci Report* 8 (2018) 5073.
<https://doi.org/10.1038/s41598-018-23348-9>
- [35] Ghanbari A, Khordad R, Taghizadeh F, Influence of Coulomb term on thermal properties of fluorine. *Chem Phys Lett* 801 (2022) 139725.
<https://doi.org/10.1016/j.cplett.2022.139725>
- [36] Sadeghi E, Naghdi E, Effect of electric and magnetic field on impurity binding energy in zinc-blend symmetric InGaN/GaN multiple quantum dots. *Nano Converg* 1 (2014) 25. <https://doi.org/10.1186/s40580-014-0025-3>

-
- [37] Chen T, Xie W, Liang S, Optical and electronic properties of a two-dimensional quantum dot with an impurity. *J Lumin* 139 (2013) 64-68.
<https://doi.org/10.1016/j.jlumin.2013.02.030>
- [38] Dong S. H, Lozada-Cassou M, Yu J, Angeles F. J, Rivera A. L, Hidden symmetries and thermodynamic properties for a harmonic oscillator plus an inverse square potential. *Int J Quant Chem* 107 (2007) 366-371.
<https://doi.org/10.1002/qua.21103>
- [39] Mikhail I. F. I, Shafee A. M, Optical absorption in a disk-shaped quantum dot in the presence of an impurity. *Physica B* 507 (2017) 142.
<https://doi.org/10.1016/j.physb.2016.11.027>
- [40] Ghanbari A, Khordad R, Taghizadeh F, Nasirizadeh I, Edet C. O, Ali N, Impurity effect on thermal properties of tuned quantum dot/ring systems. *Chem Phys Lett* 806 (2022) 140000.
<https://doi.org/10.1016/j.cplett.2022.140000>
- [41] Pal S, Ghosh M, Duque C. A, Impurity related optical properties in tuned quantum dot/ring systems. *Philos Mag* 99 (2019) 2457.
<https://doi.org/10.1080/14786435.2019.1619949>